

Medical & Biological Engineering & Computing

Simulation Study of Transcatheter Heart Valve Implantation in Patients with Stenotic Bicuspid Aortic Valve --Manuscript Draft--

Manuscript Number:	MBEC-D-19-00568R2	
Full Title:	Simulation Study of Transcatheter Heart Valve Implantation in Patients with Stenotic Bicuspid Aortic Valve	
Article Type:	Original article	
Keywords:	transcatheter aortic valve implantation; bicuspid aortic valve; finite-element analysis; fluid-solid interaction	
Corresponding Author:	Salvatore Pasta Universita degli Studi di Palermo palermo, ITALY	
Corresponding Author Secondary Information:		
Corresponding Author's Institution:	Universita degli Studi di Palermo	
Corresponding Author's Secondary Institution:		
First Author:	Salvatore Pasta	
First Author Secondary Information:		
Order of Authors:	Salvatore Pasta	
	Stefano Cannata	
	Giovanni Gentile	
	Marzio Di Giuseppe	
	Federica Cosentino	
	Francesca Pasta	
	Valentina Agnese	
	Diego Bellavia	
	Giuseppe M Raffa	
	Michele Pilato	
Caterina Gandolfo		
Order of Authors Secondary Information:		
Funding Information:	Ministero della Salute (GR-2011-02348129)	Prof Salvatore Pasta
Abstract:	<p>Bicuspid aortic valve (BAV) anatomy has routinely been considered an exclusion in the setting of transcatheter aortic valve implantation (TAVI) because of the large dimension of the aortic annulus having a more calcified, bulky, and irregular shape. The study aims to develop a patient-specific computational framework to virtually simulate TAVI in stenotic BAV patients using the Edwards SAPIEN 3 valve (S3) and its improved version SAPIEN 3 Ultra and quantify stent frame deformity as well as the severity of paravalvular leakage (PVL). Specifically, the aortic root anatomy of n.9 BAV patients who underwent TAVI was reconstructed from pre-operative CT imaging. Crimping and deployment of S3 frame was performed and then followed by fluid-solid interaction analysis to simulate valve leaflet dynamics throughout the entire cardiac cycle. Modeling revealed that the S3 stent frame expanded well on BAV anatomy with an elliptical shape at the aortic annulus. Comparison of predicted S3 deformity as assessed by eccentricity and expansion indices demonstrated a good agreement with</p>	

	<p>the measurement obtained from CT imaging. Blood particle flow analysis demonstrated a backward blood jet during diastole whereas the predicted PVL flows corresponded well with those determined by transesophageal echocardiography. This study represents a further step towards the use of personalized simulations to virtually plan TAVI, aiming at improving not only the efficacy of the implantation, but also the exploration of "off-label" applications as the TAVI in the setting of BAV patients.</p>
<p>Response to Reviewers:</p>	<p>Reviewer #1</p> <p>We thank the reviewer for his or her valuable consideration about our study. We have taken comments into careful consideration when preparing the revised manuscript and feel that the critiques led directly to an improved submission. We hope that the reviewer agrees. All changes in the text are highlighted in yellow.</p> <p>Introduction</p> <p>Q1: "...The mesh shown in Fig. 1 for the valve leaflet was not used for FEA" - If this is the case, can the authors please present the meshed leaflet as it was used in the FEA?</p> <p>Reply: Fig.1 was adjusted and now the inset of Fig1B shows the mesh with element density adopted for FEA.</p> <p>Results</p> <p>Q1: The video is indeed good. However, it is not satisfied and doesn't sufficiently visualize the flow through the TAVI, nor the leakage. Please edit fig.8 as requested, to represent the velocity magnitudes in the same manner as seen in the video, and present the leakage as well.</p> <p>Reply: Fig.8 was edited to show the velocity magnitude in the same way as the video. Please note that we cannot obtain the maps of flow velocity as we used SPH and thus have the velocity value of each particle.</p> <p>Discussion</p> <p>Q1: There is in literature only one investigation based on computational flow analysis to assess PVL in bicuspid patients treated with the newer generation of bioprosthesis [6] (ie, the Medtronic CoreValve Evolut R"- As mentioned before, this statement is not accurate, there are already few published studies on TAVR in BAVs and PVL calculation, that the authors can compare to. It also contradicts the sentence: "With regards to stenotic bicuspid leaflets, Levon et al. [20] simulated the TAVI deployment in an ideal aortic root geometry of a calcified BAV to assess PVL and asymmetric stent expansion."</p> <p>Reply: Fixed with the following sentence:</p> <p>"With regards to the self-expandable Medtronic CoreValve Evolut R, Brouwer et al. [6] carried out computational flow analyses to assess PVL in bicuspid patients with severe aortic valve stenosis."</p> <p>Minor Comment: ""...With regards to stenotic bicuspid leaflets, Levon et al. [18] simulated the TAVI.." - There is a mismatch between the reference number to the author name.</p> <p>Reply: Fixed</p>

[Click here to view linked References](#)

Simulation Study of Transcatheter Heart Valve Implantation in Patients with Stenotic Bicuspid Aortic Valve

Salvatore Pasta¹, Stefano Cannata², Giovanni Gentile³, Marzio Di Giuseppe⁴, Federica Cosentino⁴, Francesca Pasta⁵, Valentina Agnese², Diego Bellavia², Giuseppe M Raffa², Michele Pilato², Caterina Gandolfo²

¹ Department of Engineering, viale delle Scienze, Ed.8, 90128, Università degli Studi di Palermo, Palermo Italy

² Department for the Treatment and Study of Cardiothoracic Diseases and Cardiothoracic Transplantation, IRCCS-ISMETT, via Tricomi n.5, 90127, Palermo, Italy

³ Department of Diagnostic and Therapeutic Services, Radiology Unit, IRCCS-ISMETT, Palermo, Italy

³ Department of Department of Health Promotion, Mother and Child Care, Internal Medicine and Medical Specialties, University of Palermo, Palermo, Italy

⁴ Biomedicina, Neuroscienze e Diagnostica Avanzata, via del Vespro, n.129, 90128, Università degli Studi di Palermo, Palermo, Italy

Conflict of interest: none

* Corresponding author:

Salvatore Pasta, PhD

Professor of Industrial Bioengineering,

Department of Engineering

University of Palermo

Phone: +39 091 3815681

FAX: +39 091 3815682

e-mail: salvatore.pasta@unipa.it

ABSTRACT

Bicuspid aortic valve (BAV) anatomy has routinely been considered an exclusion in the setting of transcatheter aortic valve implantation (TAVI) because of the large dimension of the aortic annulus having a more calcified, bulky, and irregular shape. The study aims to develop a patient-specific computational framework to virtually simulate TAVI in stenotic BAV patients using the Edwards SAPIEN 3 valve (S3) and its improved version SAPIEN 3 Ultra and quantify stent frame deformity as well as the severity of paravalvular leakage (PVL). Specifically, the aortic root anatomy of n.9 BAV patients who underwent TAVI was reconstructed from pre-operative CT imaging. Crimping and deployment of S3 frame was performed and then followed by fluid-solid interaction analysis to simulate valve leaflet dynamics throughout the entire cardiac cycle. Modeling revealed that the S3 stent frame expanded well on BAV anatomy with an elliptical shape at the aortic annulus. Comparison of predicted S3 deformity as assessed by eccentricity and expansion indices demonstrated a good agreement with the measurement obtained from CT imaging. Blood particle flow analysis demonstrated a backward blood jet during diastole whereas the predicted PVL flows corresponded well with those determined by transesophageal echocardiography. This study represents a further step towards the use of personalized simulations to virtually plan TAVI, aiming at improving not only the efficacy of the implantation, but also the exploration of “off-label” applications as the TAVI in the setting of BAV patients.

Keywords: transcatheter aortic valve implantation; bicuspid aortic valve; finite-element analysis; fluid-solid interaction

INTRODUCTION

Bicuspid aortic valve (BAV) is among the most common congenital cardiac abnormalities and is associated with high risk of aortic dilatation, rapid leaflet degeneration and calcification, leading to dysfunction of the aortic valve [41]. Stenosis of bicuspid valve leaflets typically occurs at a younger age than that of individuals with the morphological-normal tricuspid aortic valve. Indeed, BAVs are more vulnerable to develop aortic stenosis due to increased mechanical stress and have a predisposition to calcium formation [20]. Nevertheless, BAV remains a significant cause of mortality and morbidity in elderly patients having conventionally high surgical risk [37,11].

Transcatheter aortic valve implantation (TAVI) for the treatment of the aortic stenosis in high-risk patients has emerged as a promising therapeutic alternative to conventional surgical repair of the tricuspid aortic valve. There is however a paucity of data for TAVI in the setting of stenotic BAV patients because the elliptical shape of the bicuspid annulus was considered an exclusion for TAVI [42,45]. Therefore, bicuspid patients were not included in clinical trials to assess TAVI feasibility and outcome. Specific anatomical characteristics, not only limited to a baseline elliptical annulus, predisposes BAV patients to complications such as valve malposition or malfunction, incomplete valve deployment, severe paravalvular leakage (PVL) and annulus rupture. Early reports have shown that TAVI may be a feasible option for the bicuspid patient [33,44,38] and analyzed the clinical performance of the first-generation of TAVI devices with somewhat disappointing outcomes related to the presence of PVL. With the expansion of TAVI into lower-risk patient groups and thanks to the design advances of the new generation of bioprosthesis, successful TAVI procedures in stenotic BAVs have been recently reported [36,18] and suggested that a relative proportion of BAV patients is expected to be treated in the next years. The Edwards SAPIEN 3 valve and its improved version SAPIEN 3 Ultra are newer-generation devices fabricated with an outer sealing skirt having the potential for a better

conformation to the oval shape and valve orifices of bicuspid patients, thus reducing the risk of leakage and potentially improving the outcome in BAV patients undergoing TAVI.

In this context, computational modeling has been employed to determine the biomechanical interaction of TAVI devices with native aortic valve leaflets [30,31,40,9]. Recently, more complex computational approaches based on fluid-solid interaction (FSI) were adopted to simulate TAVI and assess PVL in real clinical cases [4,24]. With regards to stenotic bicuspid leaflets, Levon et al. [21] simulated the TAVI deployment in an ideal aortic root geometry of a calcified BAV to assess PVL and asymmetric stent expansion.

This study aimed to develop a computational framework to simulate TAVI in stenotic bicuspid patients using a patient-specific computational framework, including finite-element analysis of S3 deployment to determine eccentricity and expansion of the prosthetic heart valve and fluid-solid interaction analysis based on smoothed particle hydrodynamic (SPH) method to assess the severity of PVL. Comparison of computational variables with those measured from post-TAVI computed tomography (CT) and transesophageal echocardiography (TEE) was carried out for a patient study group of nine bicuspid patients who underwent TAVI.

METHODS

TAVI procedure and bicuspid classification

We retrospectively included n.9 patients with severe stenosis of BAV treated by TAVI as discussed by the Heart Team on the basis of clinical considerations of the risk profile of each case. Stenotic BAVs were treated with the S3 and S3 Ultra (Edwards Lifesciences, Irvine, CA, USA) using device diameters ranging from 23 mm to 29 mm. TAVI procedure was performed according to clinical guidelines *via* transfemoral access as previously described [14]. Annulus dimensions used for S3 sizing were based on CT measurements and TEE assessment. CT

scans were retro-reconstructed using a multisegment reconstruction algorithm with resolution of 0.625mm in the z-axis. Successful implantation of S3 device was estimated by post-TAVI CT imaging to evaluate the correct positioning and deployment as well as TEE functional imaging to determine hemodynamic performance of S3 transcatheter heart valve.

Valve phenotype was classified as previously reported by Sievers et al. [39] according to the number of cusps and the presence of raphes, as well as the spatial position and symmetry of raphes and cusps. Type 0 was assigned to “pure” bicuspid morphologies characterized by the presence of 2 symmetric leaflets/cusps and 1 commissure without evidence of a raphe. Type 1 was assigned to valve morphologies with 1 raphe, and Type 2 when 2 raphes were present. Phenotypic classification was made by an experienced radiologist using CT images reconstructed parallel to the aortic valve plane. Table 1 summarizes clinical demographic data, BAV phenotype and baseline CT and TEE measurements for each patient.

Computational Analysis

The proposed computational framework (see Figure 1) to simulate TAVI in BAV patients consisted of the following steps:

1. Patient-specific reconstructions of aortic root and calcification geometries from CT images as well as medical imaging measurements of native BAV leaflets;
2. Parametric modeling of native BAV leaflets using 3rd-order NURBS curves as described by our group for the bicuspid aortopathy [34] and then meshing of each component of TAVI model;
3. Simulation of pre-TAVI scenario by imposing a uniform transmural pressure difference on BAV leaflets;
4. Crimping and deployment of S3 frame by means of a moving cylindrical surface and then mapping of the S3 prosthetic valve leaflets onto deployed S3 stent frame;

5. FSI analysis by SPH of implanted S3 device to simulate valve leaflet dynamics throughout the entire cardiac cycle.

Virtual Aortic Root Model

Pre-TAVI CT images were processed by Mimics (v.21, Materialise, Belgium) to reconstruct the aortic root anatomy and calcific plaques using different greyvalues and multiple masks. Specifically, aortic root reconstructions from the left ventricular outflow tract ending to the mid-ascending aorta were carried out using semi-automatic thresholding of the contrast-enhanced images, cropping and morphologic operations. Using different Hounsfield unit thresholds, calcifications from the surrounding healthy tissue were extracted in terms of both spatial location and dimension. Once the segmented regions were extracted, the aortic root and calcific plaques were independently exported as stereolithographic (STL) files for meshing.

Since native BAV leaflet geometry was not clearly visible at CT scan, a parametric modeling tool based on both Rhino CAD software (Rhinoceros v.5.5, McNeel & associates) and BAV-related anatomic measures was used to design native bicuspid valve leaflets according to a protocol developed by our group for the bicuspid aortopathy [34]. In brief, the cusp-to-commissure distances and their characteristic angles were measured for each BAV patients in the aortic valve plane. Then, two 3rd-order NURBS curves interpolating commissures were adopted to model the free edge of BAV leaflets while the bending of each leaflet was controlled using three control points (see Figure 1B). To model leaflet attachments, a second set of 3rd-order NURBS curves were build and controlled by five control points to adjust the position of each leaflet-to-sinus attachment. Then, NURBS curves were constrained to the aortic root surface by curve-to-surface projection, assuming as projection direction the vector between the coaptation center and the end points of BAV characteristic lengths on annulus shape. Using these bounding curves, native bicuspid leaflets were modeled by a multi-patch network of NURBS surfaces.

Using ICEM meshing software (Ansys v.18, ANSYS, Inc.), the aortic root luminal surface and the native BAV leaflet surface were discretized with structured quadrilateral shell elements with reduced integration (see Table 2). Calcific plaques were meshed by a combination of hexahedral and tetrahedral solid elements (element size of 0.1 mm). Kinematic coupling constraint coupling was used for the interaction between calcifications and valve leaflets.

Transcatheter Heart Valve Model

The Edwards Lifesciences SAPIEN 3 is manufactured by a cobalt-chromium alloy frame with four cells for each row and twelve columns where three-sutured bovine pericardial leaflets are anchored [5]. The S3 device is designed with an outer sealing skirt to minimize PVL at inflow portion of the transcatheter heart valve. The most recent advancement is the S3 Ultra showing a 40% increased outer skirt height as compared to that of the S3 design while the frame was maintained.

The geometrical model of 26 mm S3 frame was acquired with a high-resolution micro-CT scanner and then a general reverse engineering approach was adopted to obtain the CAD model of the prosthetic heart valve (Figure 2). Nearly 60,000 structured-hexahedral solid elements with reduced integration were used to discretize the S3 frame. The sealing skirt was modeled using a cylindrical surface from the bottom to the first row for the S3 and from the bottom to the second row for the S3 Ultra [13]. This cylindrical surface was meshed with structured-quadrilateral shell elements with size of 0.3 mm. Prosthetic valve leaflets were modeled using a general 3D parametric geometry of the native aortic valve leaflet [3]. The 23 mm and 29 mm S3 stent frames were obtained by scaling that of 26mm S3 frame.

Material Models

For the sake of simplicity, the aortic root wall and native BAV leaflets were modeled as hyperelastic and isotropic materials using a two-term Yeoh constitutive relation as assumed in other studies [12,31,35]. The form of strain energy function is:

$$W = C_{10}(I_B - 3) + C_{20}(I_B - 3)^2 \quad \text{Eq.1}$$

where I_B is the first invariant of the Left Cauchy-Green tensor \mathbf{B} ($\mathbf{B} = \mathbf{F}\mathbf{F}^T$, where \mathbf{F} is the deformation gradient tensor), and C_{10} and C_{20} are material model descriptors indicative of mechanical properties of the aortic wall. Aortic root and native BAV leaflets were assumed with a uniform thickness of 2.0 and 0.5 mm, respectively. Linear elastic material properties were adopted to model calcified plaques while Von Mises plasticity and isotropic hardening was used for the S3 stent frame [31]. An elasto-plastic stress-strain model was used for the cylindrical surface representing the outer sealing skirt of S3 device (surface thickness of 0.1 mm) [19]. For the prosthetic valve leaflets, the constitutive characteristic of bovine pericardium was modeled with a linear-elastic material and uniform thickness of 0.4 mm as previously documented by Xiong et al [43]. Table 2 describes the material parameters for each component of TAVI simulation in BAV.

FEA of TAVI in BAV patients

Numerical analysis of TAVI procedure is non-linear problems including large deformation and complex contacts so that Abaqus/Explicit solver (Abaqus 2018, Dassault Systemes) was adopted to model TAVI as a quasi-static process [32]. Energy was monitored to ensure the ratio of kinetic energy to internal energy remains less than 10%. Adequate time step (minimal value of 10^{-6} s) was applied while an element-by-element stable time increment estimate, coupled with a “variable mass scaling technique,” reduced the computational cost of each simulation. Contacts among components were defined according to the general contact algorithm available in Abaqus/Explicit. Simulations were performed on a 24 CPUs workstation, and solutions were obtained after 3 days.

The pre-TAVI scenario was obtained applying a pressure differential waveform (ie, a pressure difference between the ventricle and the aorta) on the closed native bicuspid surface as done by Gnyaneshwar et al [15]. This allowed us to have enough space for the position of both S3 frame and cannula without penetration among components (Figure 1D).

Following the approach developed by Morganti et al. [31], the S3 device was crimped by a rigid cylindrical surface gradually moved along the radial direction from the initial diameter of S3 (ie, 23, 26 or 29 mm) to the final diameter of 6 mm (time period of 0.03 s). This surface was meshed using 1,500 structured-quadrilateral surface elements with reduced integration and material density of 7000 kg/m³. A frictionless contact is defined between the crimping surface and the S3 stent frame while tie contact conditions were used to fix the cylindrical surface of the sealing skirt to the stent frame. The deformed configuration of S3 device was imported into the aortic root model, taking into account the stress state resulting from the crimping simulation (see Figure 1E). For each patient, the prosthetic heart valve was positioned according to the implantation depth and tilt angle decided by the Heart Team during pre-TAVI planning procedure done in the hybrid operating room of our hospital institution.

Expansion of S3 stent frame was simulated by the radial displacement of a rigid cylindrical surface representing the wall of the expanding balloon (time period of 0.1 s) [12,31]. This is a valid assumption since angiography shows negligible axis rotation and translation during stent expansion. The cylindrical surface is enlarged from the initial diameter of 6 mm to the nominal diameter of S3 frame. Frictionless contact was enabled between the cylindrical expanding surface and the S3 stent frame, which was allowed to be in contact with other components (ie, aortic root, native BAV leaflet and calcific plaque).

As boundary conditions, the proximal and distal ends of the aortic root wall were fixed in longitudinal and circumferential directions of the vessel using cylindrical coordinate system. No boundary conditions were directly applied to the S3 stent frame, which was driven by the cylindrical expanding surface and contact interaction. After each expansion (Step 1), an elastic recoil of S3 device (time period of 0.02 s) was allowed by the release of the cylindrical surface (Step 2). Prosthetic valve leaflets were mapped onto the implanted S3 stent frame at initial stress-free closed configuration as described by Auricchio et al. [2] (Figure 1F).

SPH Modeling

A detailed description of SPH fundamentals can be found in Monaghan et al. [29]. This numerical technique is advantageous as compared to coupled Eulerian-Lagrangian methods in tracking free surface boundaries, handling small material-to-void ratios, and modeling extreme deformation. The latter capability makes it ideal for simulating the fluid behavior during valve closure/opening as done in other SPH studies for the mitral and aortic valves [25,26]. SPH is a meshless numerical method defining a body by a collection of points, instead of using nodes and elements. In this study, the SPH method implemented in Abaqus 2018 adopted a cubic spline kernel function (W) for particle-to-particle interpolation. Particles can contact Lagrangian bodies using the general Abaqus/Explicit contact algorithm. Under these conditions, the general form of conservation of mass and momentum for the SPH scheme are:

$$\frac{d\rho_a}{dt} = \sum_b m_b \mathbf{v}_{ab} \cdot \nabla_a W_{ab} \quad \text{Eq.2}$$

$$\frac{d\mathbf{v}_a}{dt} = - \sum_b m_b \left(\frac{P_a - P_b}{\rho_a \rho_b} \right) \nabla_a W_{ab} + \sum_b m_b \frac{(\mu_a - \mu_b)}{\rho_a \rho_b r_{ab}^2} \mathbf{r}_{ab} \cdot \nabla_a W_{ab} \quad \text{Eq.3}$$

where $\nabla_a W_{ab}$ is the gradient of the kernel function regarding the coordinates of given particle 'a', $\mathbf{v}_{ab} = \mathbf{v}_a - \mathbf{v}_b$ is the relative velocity vector between particles 'a' and 'b', P is the blood

pressure, μ and ρ are the dynamic viscosity and density of the blood fluid, m is the mass and r is the position of particle with subscripts denoting adjoining particles.

In this study, we set a reference density of 1060 kg/m^3 and viscosity of 0.0035 Pa s for blood properties using the pressure-density relation governed by the linear Hugoniot equation of state. For the blood flow in the aorta, the speed of sound is high compared to the bulk velocity of the blood so that an artificial sound speed of $c_0=145 \text{ m/s}$ was employed to avoid very small computational time steps while keeping density fluctuations within a small range and thus maintaining the incompressible flow behavior. Particles were uniformly distributed in the fluid domain with a spatial resolution of 0.5 mm in agreement with mesh sensitivity analysis carried out by Mao et al. [26] who studied the mechanics and hemodynamic of a transcatheter aortic valve in an ideal model by SPH method. Two rigid plates were used to apply pressure boundary conditions on the blood volume; specifically, physiological pressure waveforms were used to obtain the pressure gradient between the left ventricle and aorta (Figure 1G). The proximal and distal ends of the aortic root were sufficiently extended to ensure a fully developed flow. The beginning of the ejection phase was selected as the starting point of the simulation. For each BAV patient, two cardiac cycles each of 0.8s were carried out and the particle velocity field from the second cycle was analyzed. Contacts were enabled between particles and other components to allow fluid-solid interaction.

Quantified Variables

Morphological, structural and hemodynamic variables were quantified from post-TAVI CT and TEE imaging modalities and then compared to those predicted by computational analysis. Using both CT scans and TAVI simulations, each S3 was assessed at five cross-sectional levels—inflow, annulus, mid, sinus, and outflow—following the reformatting of the aortic root in the short-axis view. At each level, the minimum external valve diameter, maximum external valve

diameter, and external valve area were measured to quantify both the S3 eccentricity and expansion. The eccentricity index was calculated as: $[1 - (\text{minimum external THV diameter}/\text{maximum external THV diameter})] \times 100$ while the expansion index was expressed in relation to nominal prosthesis size as: $(\text{observed S3 external area}/\text{device area nominal size}) \times 100$. The nominal external valve areas were 406, 519, and 649 mm² for the 23, 26, and 29 mm valves, respectively. In addition, the S3 depth was measured as the distance from the inflow of the valve to the annulus level. For each TAVI simulation, the maximum of Von Mises stress was quantified at aortic annulus while the severity of aortic regurgitation over one cardiac cycle was categorized as PVL using TEE imaging and classified as minimal, moderate, or severe [17]. For each SPH simulation, degree of PVL was computed as the flow circulating into the leakage gap area between the aortic wall and S3 stent frame. Using Rhino CAD software, the leakage gap area was measured by cross-sections in the short axis view of the deformed TAVI configuration while the SPH analysis allowed to measure the mean particle velocity in the gap area.

t-test was used to compare computational variables to those measured by CT imaging. The correlation of calcific plaque volume with PVL was assessed by Pearson's analysis. Data are shown as mean \pm std, with significance set to $\alpha=0.05$.

RESULTS

From post-TAVI CT imaging, we observed that the S3 stent frame was characterized by an elliptical shape at aortic annulus to accommodate the bicuspid anatomy (major axis of 27.7mm and minor axis of 24.4mm for Case #1 as shown by Figure 3).

For the patient Case #1, Figure 4 shows the pre-TAVI configuration and the deformed configuration of S3 Ultra device with the resulting distribution of the wall stress on both the aortic root and stent frame. Aortic root stress should be ideally uniform, resembling a homogeneous

contact of S3 device with the vessel wall. However, distributions of wall stress were mostly characterized by local maxima in the contact area of the aortic root with either S3 frame or calcific plaques. At mid and sinus levels, the transcatheter heart valve exhibited pronounced deformation with stress concentrations at the intersection of each stent column. Despite S3 deformity, TEE showed normal valve function with minimal PVL and mean gradient of 16 mmHg for this patient (Figure 4C). Table 3 summarizes maxima of Von Mises wall stress at aortic annulus for each patient while the stress distribution is shown in Figure 5.

For each BAV patient, deformed configurations of implanted prosthetic heart valves are shown in Figure 6. It can be observed that the degree of S3 deformity is highly variable from patient to patients, with relevant frame distortions caused by the amount and positions of calcifications with respect to the aortic root anatomy. Case #9 had remarkable distortion of the S3 device in correspondence of the sinus of Valsalva whereas Case # 6 with a “pure” Type 0 bicuspid phenotype and large aortic annulus had an irregular expansion of the 29 mm S3 transcatheter heart valve.

Comparison of predicted eccentricity and expansion indices with those measured from CT imaging at different anatomic levels is shown in Figure 7. Specifically, the distribution of predicted eccentricity at the level of the aortic annulus differed statistically from those measured from CT imaging, with numerical simulations slightly overestimating S3-related elliptical shapes (eg, 5.4 ± 2.0 % for numerical simulations and 7.3 ± 2.4 % for CT measures, $p=0.042$). There was also a statistical difference on the expansion indices at mid-level between predicted and CT-based measurements (eg, 90.1 ± 5.5 % for numerical simulations and 87.2 ± 2.9 % for CT measures, $p=0.035$). We observed a good agreement in the distribution of eccentricity and expansion indices in other regions of S3 device, suggesting predictive capability of the proposed computational framework of TAVI procedure. The predicted S3 implantation depth agreed well

with post-TAVI CT measurements (ie, mean of 5.5 ± 1.5 mm for numerical simulations and 5.2 ± 0.8 mm for CT measures, $p=0.349$).

Particle flow motion was assessed on a cross-section through the symmetry plane of the prosthetic heart valve at ten-time instances of the entire cardiac cycle as shown by Figure 8 for the Case #3. During the ejection phase ($t = 0.1$ s and 0.2 s), a strong outward jet was developed along the axial direction with a nearly circular jet profile. Opening and closing of prosthetic valve leaflet reflected that of a well-functioning tricuspid aortic valve during heart beating (see Figure 9). At late diastole when prosthetic valve leaflets are fully closed ($t = 0.6$, 0.7 and 0.8 s), we observed a slight backward flow particle jet moving towards the left ventricular outflow tract. The velocity of blood particles flowing in the leakage gap area was evaluated to calculate the PVL for each patient (see Table 3). The highest PVL graded as moderate was observed for the BAV patient with a Type 1 BAV treated with the 26 mm S3 device (ie, Case #3). Movie 1 shows flow-colored particle motion for Case #3. A comparison revealed that the predicted PVL flow degrees were in agreement with those quantified by TEE imaging (see Table 3). At Pearson's correlation, we found a poor positive correlation between PVL and calcification volume ($R=0.53$, $p=0.137$).

DISCUSSION

This study documented a detailed analysis of TAVI in patients with stenotic BAVs to describe the early use of patient-specific computational modeling in predicting procedure feasibility. TAVI in bicuspid patients is challenging because of morphological features (not observed in the tricuspid aortic valve morphology) that make outcomes less predictable. The tendency of the S3 device to expand asymmetrically in the aortic root was predicted at several anatomic levels and then compared to that observed from post-TAVI CT imaging. Using the SPH method, the fluid-

solid interaction between blood and S3 transcatheter heart valve was simulated to compute the degree of PVL for each bicuspid patient. The predicted values of eccentricity, S3 expansion and PVL were in agreement with those measured by CT and TEE. This research suggests that numerical simulations are promising to predict several clinically relevant information of TAVI in the setting of a stenotic BAV, but validation in a larger patient population is necessary to apply it in a clinical practice.

Computational modeling taking into account patient-specific aortic root anatomies can be used to predict several variables that are of clinical interest to support decision on diseased heart valves [22,8]. Numerical simulations of TAVI demonstrated the presence of stress concentration induced by the contact between the stent and the aortic wall [31] as a major risk indicator of aortic rupture [9] as well as the impact of aortic root anatomy [12], calcification patterns [40] and native leaflets [3] on the outcome of TAVI. However, these studies focused on patients with the tricuspid aortic valve to simulate the implantation of both Edwards SAPIEN XT and Medtronic Corevalve. With regards to the self-expandable Medtronic CoreValve Evolut R, Brouwer et al. [6] carried out computational flow analyses to assess PVL in bicuspid patients with severe aortic valve stenosis.

Although TAVI has emerged as a promising alternative strategy to surgery in patients with a stenotic aortic valve and contraindications to open-chest surgery, the bicuspid anatomic phenotype has been considered an exclusion in most clinical trials because of the risk of uneven expansion and subsequent malfunction of the prosthetic heart valve [23]. Individuals with BAV usually have larger left ventricular outflow tract and annulus, and dilated ascending aorta than TAV patients, as well as a greater aortic valve calcium volume as assessed by CT imaging. High rate of PVL in BAV patients have been reported with the first generation of bioprosthesis [33,38,44]. Notwithstanding, several recent investigations highlighted the

feasibility of TAVI in the setting of stenotic BAVs [36,18]. Using the S3 device, Arai et al. [1] found comparable degree of PVL between bicuspid and tricuspid patients when leak was graded equal or greater than mild. It should be however considered that a mild degree of PVL after TAVI is predictor of adverse events. In a large series, Hayashida and collaborators [16] evinced no significant differences in the device success rate, risk of annulus rupture and valve migration of BAV patients versus tricuspid patients. The feasibility and safety of TAVI in BAVs was likely a consequence of the design advancements incorporated by the newer generation of TAVI devices that partially overcome some of limitations encountered in treating BAV. To our knowledge, this is the first study using the S3 device and confirmed clinical evidence of an elliptical expansion induced by the oval bicuspid annulus shape. Using the eccentricity and expansion indexes, the S3 deformity was found in agreement with measurements from post-TAVI CT imaging and was found highly depending on patient anatomy. The worse scenario was observed when the S3 was virtually implanted on the “pure” bicuspid phenotype while the patient cases with the functional BAVs presented less S3 deformity, likely taking an intermediate stance between the congenital bicuspid valve and the tricuspid valve. Device deformity is not only caused by the presence of a baseline annulus eccentricity of bicuspid patients but is also caused by heavy calcification and calcified raphe.

Whether calcification is a predictor of the grade of PVL is still debatable as some groups have shown significant correlation [10] while other studies did not [28]. From an engineering point of view, our findings highlighted that a heavy focal calcification causes asymmetric expansion of S3 stent frame at mid and sinus levels, likely portending to the onset of PVL. However, the occurrence of post-TAVI leakage is multifactorial and strongly depending on the complex interaction between the S3 and the aortic wall, including factors related to native leaflets, calcification and aortic annulus, deployment height, and device/annulus sizing ratio. This could explain the poor linear association between calcification volume and the PVL flow found in this

study by Pearson analysis ($R=0.53$, $p=0.137$). In the future, we will perform statistical shape analysis for identifying the principal modes of geometric variations of calcified bicuspid leaflets to better reveal the mechanistic link between the calcium burden and the amount of leakage. This however requires a large patient study group that is not easy to achieve in BAV patients because TAVI in this population is often an “off-label” application, with limited patient cases for reference heart centers.

It is expected that the increased sealing skirt height of S3 Ultra would ideally reduce the PVL severity after TAVI. We found a slightly reduced PVL flows for the Case #8 and #9 treated by the S3 Ultra with respect to patients with the S3 device, and this is likely a consequence of the increased skirt height of the S3 Ultra. Using computational fluid dynamic, Mao et al. [27] examined the PVL flow resulting from different deployment heights of the newer Medtronic CoreValve Evolut R in a TAV patient. They found that lower deployment helps to reduce PVL (as for our Case #9 with depth of 8.9 mm) and that the majority of regurgitant jets originates right below the native leaflets. Additionally, because of the scallop shape of the skirt, the PVL differences due to tricuspid orientation can be as large as 40% among simulated deployment heights. They also demonstrated that computational fluid analyses are warrant to accurately calculate the leaking flow through the irregular gaps between the aortic root and the heart valve. To date, most of the SPH implementation studies are focused on the blood flow of the heart valves and/or the left ventricle and are validated with benchmark cases [25,26]. The comparison between SPH findings, traditional CFD method, and echocardiography data showed a good quantitative agreement [7]. With regards to the validation of blood flow and PVL predictions, the particle flow patterns here reported (see Figure 8 and Movie 1) are qualitatively in agreement with those determined by CFD reported by Mao et al. [27] and Brouwer et al. [6] for TAVI. In this study, the lack of velocity values over the cardiac cycle from clinical data did not allow to confirm the simulated velocities in the aortic root. In forthcoming studies, we aim to thoroughly validate

SPH-related flow results against TEE imaging continuously gathered over different steps of the cardiac cycle.

Beyond numerical issues like constitutive modeling of the aortic wall, expansion by radial displacement rather than balloon inflation and the lack of validation of SPH mesh, the detailed analysis of S3 eccentricity, expansion and PVL has revealed insights on TAVI in stenotic bicuspid patients that cannot be obtained by conventional CT and TEE examinations. This study represents a further step towards the use of personalized simulations for the virtual planning of TAVI, aiming at improving not only the efficacy of the heart valve implantation, but also the exploration of borderline application as the TAVI in bicuspid patients. The computational framework here proposed may also assist the design of next-generation of prosthetic heart valves by means of *in-silico* clinical trials, thereby reducing the time-to-market application.

ACKNOWLEDGMENTS

This work was supported by a “Ricerca Finalizzata” grant from the Italian Ministry of Health (GR-2011-02348129) to Salvatore Pasta.

CONFLICT OF INTEREST

The authors declare that they have no conflict of interest.

REFERENCES

1. Arai T, Lefevre T, Hovasse T, Morice MC, Romano M, Benamer H, Garot P, Hayashida K, Bouvier E, Chevalier B (2017) The feasibility of transcatheter aortic valve implantation using the Edwards SAPIEN 3 for patients with severe bicuspid aortic stenosis. *J Cardiol* 70:220-224. doi:10.1016/j.jjcc.2016.12.009
2. Auricchio F, Conti M, Morganti S, Reali A (2014) Simulation of transcatheter aortic valve implantation: a patient-specific finite element approach. *Computer methods in biomechanics and biomedical engineering* 17:1347-1357. doi:10.1080/10255842.2012.746676
3. Bailey J, Curzen N, Bressloff NW (2016) Assessing the impact of including leaflets in the simulation of TAVI deployment into a patient-specific aortic root. *Computer methods in biomechanics and biomedical engineering* 19:733-744. doi:10.1080/10255842.2015.1058928
4. Bianchi M, Marom G, Ghosh RP, Rotman OM, Parikh P, Gruberg L, Bluestein D (2019) Patient-specific simulation of transcatheter aortic valve replacement: impact of deployment options on paravalvular leakage. *Biomechanics and modeling in mechanobiology* 18:435-451. doi:10.1007/s10237-018-1094-8
5. Binder RK, Rodes-Cabau J, Wood DA, Mok M, Leipsic J, De Laroche R, Toggweiler S, Dumont E, Freeman M, Willson AB, Webb JG (2013) Transcatheter aortic valve replacement with the SAPIEN 3: a new balloon-expandable transcatheter heart valve. *JACC Cardiovascular interventions* 6:293-300. doi:10.1016/j.jcin.2012.09.019
6. Brouwer J, Gheorghe L, Nijenhuis VJ, Ten Berg JM, Rensing B, van der Heyden JAS, Swaans MJ (2018) Insight on patient specific computer modeling of transcatheter aortic valve implantation in patients with bicuspid aortic valve disease. *Catheter Cardiovasc Interv.* doi:10.1002/ccd.27990
7. Caballero A, Mao W, Liang L, Oshinski J, Primiano C, McKay R, Kodali S, Sun W (2017) Modeling Left Ventricular Blood Flow Using Smoothed Particle Hydrodynamics. *Cardiovasc Eng Technol* 8:465-479. doi:10.1007/s13239-017-0324-z

8. D'Ancona G, Amaducci A, Rinaudo A, Pasta S, Follis F, Pilato M, Baglini R (2013) Haemodynamic predictors of a penetrating atherosclerotic ulcer rupture using fluid-structure interaction analysis. *Interactive cardiovascular and thoracic surgery* 17:576-578.
doi:10.1093/icvts/ivt245
9. Eker A, Sozzi FB, Civaia F, Bourlon F (2012) Aortic annulus rupture during transcatheter aortic valve implantation: safe aortic root replacement. *Eur J Cardiothorac Surg* 41:1205.
doi:10.1093/ejcts/ezr146
10. Ewe SH, Ng AC, Schuijff JD, van der Kley F, Colli A, Palmén M, de Weger A, Marsan NA, Holman ER, de Roos A, Schalij MJ, Bax JJ, Delgado V (2011) Location and severity of aortic valve calcium and implications for aortic regurgitation after transcatheter aortic valve implantation. *Am J Cardiol* 108:1470-1477. doi:10.1016/j.amjcard.2011.07.007
11. Fedak PW, Verma S, David TE, Leask RL, Weisel RD, Butany J (2002) Clinical and pathophysiological implications of a bicuspid aortic valve. *Circulation* 106:900-904
12. Finotello A, Morganti S, Auricchio F (2017) Finite element analysis of TAVI: Impact of native aortic root computational modeling strategies on simulation outcomes. *Medical Engineering & Physics* 47:2-12. doi:10.1016/j.medengphy.2017.06.045
13. Gandolfo C, Agnese V, Bellavia D, Gentile G, Raffa GM, Romano G, Clemenza F, Pilato M, Pasta S (2018) Modeling Transcatheter Aortic Valve Implantation in a Bicuspid Aortic Valve Patient. *The Journal of heart valve disease* 27
14. Gandolfo C, Turrisi M, Follis F, Clemenza F, Falletta C, Gentile G, Liotta R, Raffa GM, Pilato M (2018) Acute Obstructive Thrombosis of Sapien 3 Valve After Valve-in-Valve Transcatheter Aortic Valve Replacement for Degenerated Mosaic 21 Valve. *JACC Cardiovascular interventions* 11:215-217. doi:10.1016/j.jcin.2017.08.054
15. Gnyaneshwar R, Kumar RK, Balakrishnan KR (2002) Dynamic analysis of the aortic valve using a finite element model. *Ann Thorac Surg* 73:1122-1129

16. Hayashida K, Bouvier E, Lefevre T, Chevalier B, Hovasse T, Romano M, Garot P, Watanabe Y, Farge A, Donzeau-Gouge P, Cormier B, Morice MC (2013) Transcatheter Aortic Valve Implantation for Patients With Severe Bicuspid Aortic Valve Stenosis. *Circulation-Cardiovascular Interventions* 6:284-291. doi:10.1161/Circinterventions.112.000084
17. Kappetein AP, Head SJ, Genereux P, Piazza N, van Mieghem NM, Blackstone EH, Brott TG, Cohen DJ, Cutlip DE, van Es GA, Hahn RT, Kirtane AJ, Krucoff MW, Kodali S, Mack MJ, Mehran R, Rodes-Cabau J, Vranckx P, Webb JG, Windecker S, Serruys PW, Leon MB, Valve Academic Research C (2012) Updated standardized endpoint definitions for transcatheter aortic valve implantation: the Valve Academic Research Consortium-2 consensus document. *EuroIntervention : journal of EuroPCR in collaboration with the Working Group on Interventional Cardiology of the European Society of Cardiology* 8:782-795. doi:10.4244/EIJV8I7A121
18. Kawamori H, Yoon SH, Chakravarty T, Maeno Y, Kashif M, Israr S, Abramowitz Y, Mangat G, Miyasaka M, Rami T, Kazuno Y, Takahashi N, Jilaihawi H, Nakamura M, Cheng W, Friedman J, Berman D, Sharma R, Makkar RR (2018) Computed tomography characteristics of the aortic valve and the geometry of SAPIEN 3 transcatheter heart valve in patients with bicuspid aortic valve disease. *European heart journal cardiovascular Imaging* 19:1408-1418. doi:10.1093/ehjci/jex333
19. Kleinstreuer C, Li Z, Basciano CA, Seelecke S, Farber MA (2008) Computational mechanics of Nitinol stent grafts. *J Biomech* 41:2370-2378. doi:10.1016/j.jbiomech.2008.05.032
20. Kong WK, Delgado V, Poh KK, Regeer MV, Ng AC, McCormack L, Yeo TC, Shanks M, Parent S, Enache R, Popescu BA, Liang M, Yip JW, Ma LC, Kamperidis V, van Rosendael PJ, van der Velde ET, Ajmone Marsan N, Bax JJ (2017) Prognostic Implications of Raphe in Bicuspid Aortic Valve Anatomy. *JAMA cardiology* 2:285-292. doi:10.1001/jamacardio.2016.5228

21. Lavon K, Marom G, Bianchi M, Halevi R, Hamdan A, Morany A, Raanani E, Bluestein D, Haj-Ali R (2019) Biomechanical modeling of transcatheter aortic valve replacement in a stenotic bicuspid aortic valve: deployments and paravalvular leakage. *Med Biol Eng Comput* 57:2129-2143. doi:10.1007/s11517-019-02012-y
22. Lee JJ, D'Ancona G, Amaducci A, Follis F, Pilato M, Pasta S (2014) Role of computational modeling in thoracic aortic pathology: a review. *Journal of cardiac surgery* 29:653-662. doi:10.1111/jocs.12413
23. Leon MB, Smith CR, Mack M, Miller DC, Moses JW, Svensson LG, Tuzcu EM, Webb JG, Fontana GP, Makkar RR, Brown DL, Block PC, Guyton RA, Pichard AD, Bavaria JE, Herrmann HC, Douglas PS, Petersen JL, Akin JJ, Anderson WN, Wang D, Pocock S, Investigators PT (2010) Transcatheter aortic-valve implantation for aortic stenosis in patients who cannot undergo surgery. *N Engl J Med* 363:1597-1607. doi:10.1056/NEJMoa1008232
24. Luraghi G, Migliavacca F, Garcia-Gonzalez A, Chiastra C, Rossi A, Cao D, Stefanini G, Rodriguez Matas JF (2019) On the Modeling of Patient-Specific Transcatheter Aortic Valve Replacement: A Fluid-Structure Interaction Approach. *Cardiovasc Eng Technol* 10:437-455. doi:10.1007/s13239-019-00427-0
25. Mao W, Caballero A, McKay R, Primiano C, Sun W (2017) Fully-coupled fluid-structure interaction simulation of the aortic and mitral valves in a realistic 3D left ventricle model. *PLoS One* 12:e0184729. doi:10.1371/journal.pone.0184729
26. Mao W, Li K, Sun W (2016) Fluid-Structure Interaction Study of Transcatheter Aortic Valve Dynamics Using Smoothed Particle Hydrodynamics. *Cardiovasc Eng Technol* 7:374-388. doi:10.1007/s13239-016-0285-7
27. Mao W, Wang Q, Kodali S, Sun W (2018) Numerical Parametric Study of Paravalvular Leak Following a Transcatheter Aortic Valve Deployment Into a Patient-Specific Aortic Root. *Journal of biomechanical engineering* 140. doi:10.1115/1.4040457

28. Marwan M, Achenbach S, Ensminger SM, Pfleiderer T, Ropers D, Ludwig J, Weyand M, Daniel WG, Arnold M (2013) CT predictors of post-procedural aortic regurgitation in patients referred for transcatheter aortic valve implantation: an analysis of 105 patients. *The international journal of cardiovascular imaging* 29:1191-1198. doi:10.1007/s10554-013-0197-7
29. Monaghan J (2012) Smoothed particle hydrodynamics and its diverse applications. *Annual Review of Fluid Mechanics* 44 323–346
30. Morganti S, Brambilla N, Petronio AS, Reali A, Bedogni F, Auricchio F (2016) Prediction of patient-specific post-operative outcomes of TAVI procedure: The impact of the positioning strategy on valve performance. *J Biomech* 49:2513-2519. doi:10.1016/j.jbiomech.2015.10.048
31. Morganti S, Conti M, Aiello M, Valentini A, Mazzola A, Reali A, Auricchio F (2014) Simulation of transcatheter aortic valve implantation through patient-specific finite element analysis: Two clinical cases. *Journal of Biomechanics* 47:2547-2555. doi:10.1016/j.jbiomech.2014.06.007
32. Morlacchi S, Chiastra C, Gastaldi D, Pennati G, Dubini G, Migliavacca F (2011) Sequential structural and fluid dynamic numerical simulations of a stented bifurcated coronary artery. *Journal of biomechanical engineering* 133:121010. doi:10.1115/1.4005476
33. Mylotte D, Lefevre T, Watanabe Y, Sondergaard L, Windecker S, Bosmans J, Tchetché D, Kornowski R, Modine T, Sinning JM, O'Sullivan C, Barbanti M, Codner P, Dorfmeister M, Martucci J, Wenaweser P, Tamburino C, Grube E, Webb J, Lange R, Piazza N (2014) Transcatheter Aortic Valve Replacement in Bicuspid Aortic Valve Disease. *Journal of the American College of Cardiology* 63:A1939-A1939
34. Pasta S, Gentile G, Raffa GM, Scardulla F, Bellavia D, Luca A, Pilato M, Scardulla C (2017) Three-dimensional parametric modeling of bicuspid aortopathy and comparison with computational flow predictions. *Artif Organs* 41:E92-E102. doi:10.1111/aor.12866

35. Pasta S, Phillippi JA, Tsamis A, D'Amore A, Raffa GM, Pilato M, Scardulla C, Watkins SC, Wagner WR, Gleason TG, Vorp DA (2016) Constitutive modeling of ascending thoracic aortic aneurysms using microstructural parameters. *Med Eng Phys* 38:121-130.
doi:10.1016/j.medengphy.2015.11.001
36. Perlman GY, Blanke P, Dvir D, Pache G, Modine T, Barbanti M, Holy EW, Treede H, Ruile P, Neumann FJ, Gandolfo C, Saia F, Tamburino C, Mak G, Thompson C, Wood D, Leipsic J, Webb JG (2016) Bicuspid Aortic Valve Stenosis: Favorable Early Outcomes With a Next-Generation Transcatheter Heart Valve in a Multicenter Study. *JACC Cardiovascular interventions* 9:817-824. doi:10.1016/j.jcin.2016.01.002
37. Roberts WC, Janning KG, Ko JM, Filardo G, Matter GJ (2012) Frequency of congenitally bicuspid aortic valves in patients ≥ 80 years of age undergoing aortic valve replacement for aortic stenosis (with or without aortic regurgitation) and implications for transcatheter aortic valve implantation. *Am J Cardiol* 109:1632-1636. doi:10.1016/j.amjcard.2012.01.390
38. Sannino A, Cedars A, Stoler RC, Szerlip M, Mack MJ, Grayburn PA (2017) Comparison of Efficacy and Safety of Transcatheter Aortic Valve Implantation in Patients With Bicuspid Versus Tricuspid Aortic Valves. *Am J Cardiol* 120:1601-1606.
doi:10.1016/j.amjcard.2017.07.053
39. Sievers HH, Schmidtke C (2007) A classification system for the bicuspid aortic valve from 304 surgical specimens. *J Thorac Cardiovasc Surg* 133:1226-1233.
doi:10.1016/j.jtcvs.2007.01.039
40. Sturla F, Ronzoni M, Vitali M, Dimasi A, Vismara R, Preston-Maher G, Burriesci G, Votta E, Redaelli A (2016) Impact of different aortic valve calcification patterns on the outcome of transcatheter aortic valve implantation: A finite element study. *J Biomech* 49:2520-2530.
doi:10.1016/j.jbiomech.2016.03.036
41. Ward C (2000) Clinical significance of the bicuspid aortic valve. *Heart* 83:81-85

42. Wijesinghe N, Ye J, Rodes-Cabau J, Cheung A, Velianou JL, Natarajan MK, Dumont E, Nietlispach F, Gurvitch R, Wood DA, Tay E, Webb JG (2010) Transcatheter aortic valve implantation in patients with bicuspid aortic valve stenosis. *JACC Cardiovascular interventions* 3:1122-1125. doi:10.1016/j.jcin.2010.08.016
43. Xiong FL, Goetz WA, Chong CK, Chua YL, Pfeifer S, Wintermantel E, Yeo JH (2010) Finite element investigation of stentless pericardial aortic valves: relevance of leaflet geometry. *Ann Biomed Eng* 38:1908-1918. doi:10.1007/s10439-010-9940-6
44. Yoon SH, Bleiziffer S, De Backer O, Delgado V, Arai T, Ziegelmüller J, Barbanti M, Sharma R, Perlman GY, Khalique OK, Holy EW, Saraf S, Deuschl F, Fujita B, Ruile P, Neumann FJ, Pache G, Takahashi M, Kaneko H, Schmidt T, Ohno Y, Schofer N, Kong WKF, Tay E, Sugiyama D, Kawamori H, Maeno Y, Abramowitz Y, Chakravarty T, Nakamura M, Kuwata S, Yong G, Kao HL, Lee M, Kim HS, Modine T, Wong SC, Bedgoni F, Testa L, Teiger E, Butter C, Ensminger SM, Schaefer U, Dvir D, Blanke P, Leipsic J, Nietlispach F, Abdel-Wahab M, Chevalier B, Tamburino C, Hildick-Smith D, Whisenant BK, Park SJ, Colombo A, Latib A, Kodali SK, Bax JJ, Sondergaard L, Webb JG, Lefevre T, Leon MB, Makkar R (2017) Outcomes in Transcatheter Aortic Valve Replacement for Bicuspid Versus Tricuspid Aortic Valve Stenosis. *J Am Coll Cardiol* 69:2579-2589. doi:10.1016/j.jacc.2017.03.017
45. Zhao ZG, Jilaihawi H, Feng Y, Chen M (2015) Transcatheter aortic valve implantation in bicuspid anatomy. *Nature reviews Cardiology* 12:123-128. doi:10.1038/nrcardio.2014.161

Figure Legends

Figure 1: Numerical framework of TAVI in BAV patients: (A) anatomic reconstruction of the aortic root and calcification anatomies from CT images; (B) parametric modeling of native BAV leaflets; (C) meshing; (D) simulation of BAV leaflet expansion; (E) crimping and (F) deployment of S3 and then mapping of prosthetic heart valve leaflet; (G) fluid-structure interaction analysis of S3

Figure 2: CAD model of 26 mm (A) S3 device and (B) S3 Ultra Edwards Lifesciences prosthetic heart valve

Figure 3: CT images showing pre-TAVI stenotic BAV and elliptical shape of annulus (top row) and post-TAVI CT images of elliptical S3-related shape with the one side longer than other one (bottom row).

Figure 4: (A) pre-TAVI peak systolic configuration showing the opened native bicuspid leaflet; (B) deformed configuration of S3 Ultra device; (C) Continuous-wave Doppler velocity of the aortic valve showing trivial/mild PVL; map of Von Mises stress [MPa] for the (D) aortic root and (E) S3 stent frame

Figure 5: Distribution of von Mises stress [MPa] after TAVI procedure for each patient

Figure 6: Deformed configuration of S3 and S3 Ultra device for each BAV patient; red = S3 stent frame; light blue = native bicuspid valve; yellow = calcification; green = aortic root wall

Figure 7: Comparison of eccentricity and expansion indices at different anatomic levels between computational simulation (black bar) and CT measures (white bar)

Figure 8: Particle flow in a cross-section of the aortic root after TAVI implantation at different time step of the cardiac cycle the Case #3; red = S3 stent frame; light blue = native bicuspid valve; green= S3 leaflets; yellow = calcification; grey = aortic root wall

Figure 9: Motion of prosthetic heart valve leaflets during opening and closing, showing the aortic valve area at systole and coaptation at diastole; red = S3 stent frame; light blue = native bicuspid valve; green= S3 leaflets; yellow = calcification; grey = aortic root wall

Table 1: Patient demographics, echocardiographic and CT imaging as well as device size

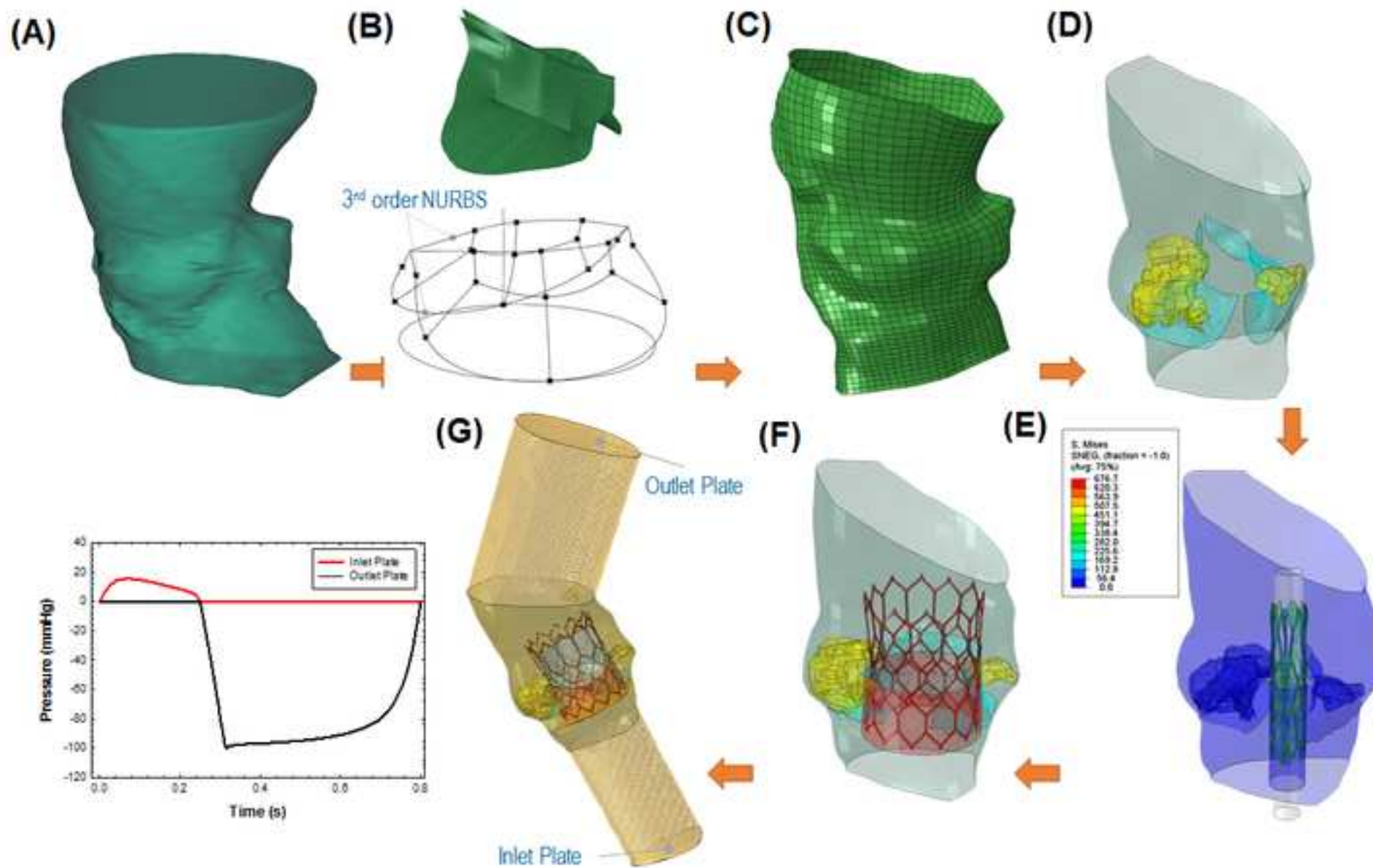
	Bicuspid Valve
Age, years	79.8±10.4
Male, %	80
Type of Bicuspid Valve	
Type 1	2
Type 1 w/raphe	5
Type 2 w/raphe	2
Pre-operative Echocardiography	
Mean Gradient, mmHg	49.1±7.2
Peak Gradient, mmHg	76.5±12.4
Aortic Valve Area, mm²	0.71±0.16
Pre-operative CT imaging	
Annulus Area, mm²	416.4±102.3
Annulus Perimeter, mm	74.2±10.7
Mean Annulus Diameter, mm	22.5±2.4
Eccentricity, %	8.1±0.9
Device	
S3 23mm	1
S3 26mm	4
S3 29mm	2
S3 Ultra 26mm	2
Post-operative Echocardiography	
Mean Gradient, mmHg	11.2±2.3
Peak Gradient, mmHg	19.8±4.0
Aortic Valve Area, mm²	0.98±0.59
Post-operative CT Imaging	
Mean S3 Depth, mm	5.2±0.8
Calcium Volume, mm³	1168.7±660.2

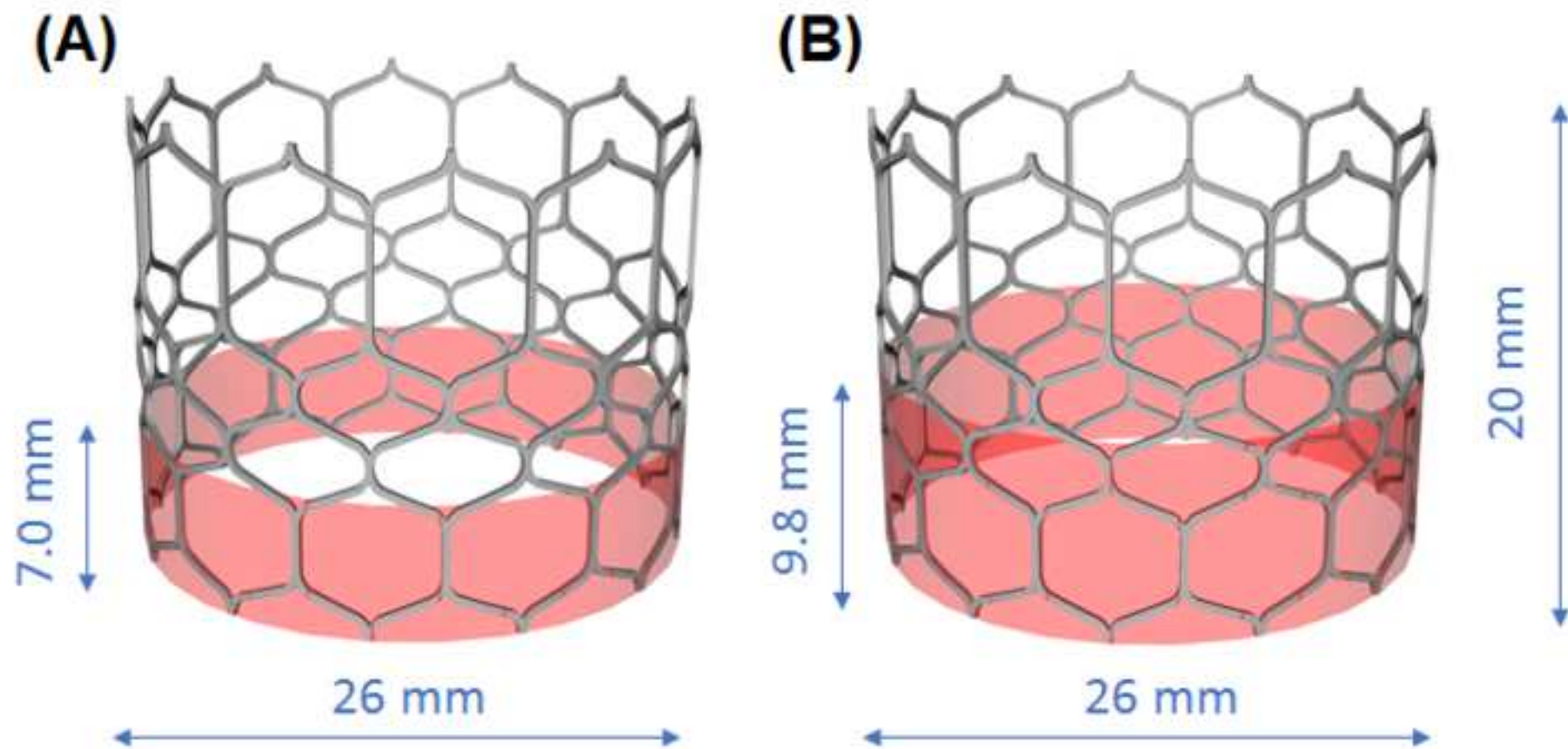
Table 2: Material parameters adopted for each component of TAVI simulation; E = Young modulus; ν = Poisson coefficient; C_{10} and C_{20} = Yeoh material parameters; σ_y = yield stress; σ_{ult} = ultimate tensile stress; ϵ_p = plastic strain; for the mesh, the range of element number is reported

	E (MPa)	ν	C_{10} (MPa)	C_{20} (MPa)	σ_y (MPa)	σ_{ult} (MPa)	ϵ_p	Density (kg/m ³)	Element Number (thousand)
Aortic Root ^[35]			0.015	0.158				1060	48.6-61.5
Native Leaflet ^[31]			0.008	0.048				1060	9.2-12.2
Calcific Plaque ^[31]	10	0.49						2000	35.2-52.3
S3 frame ^[31]	233 x10 ³	0.35			414	930	0.45	8000	59.2
Sealing Skirt ^[19]	55	0.49			6.6	6.6	0.6	8000	3.5
S3 Leaflet ^[43]	8	0.45						1060	10.5-12.5

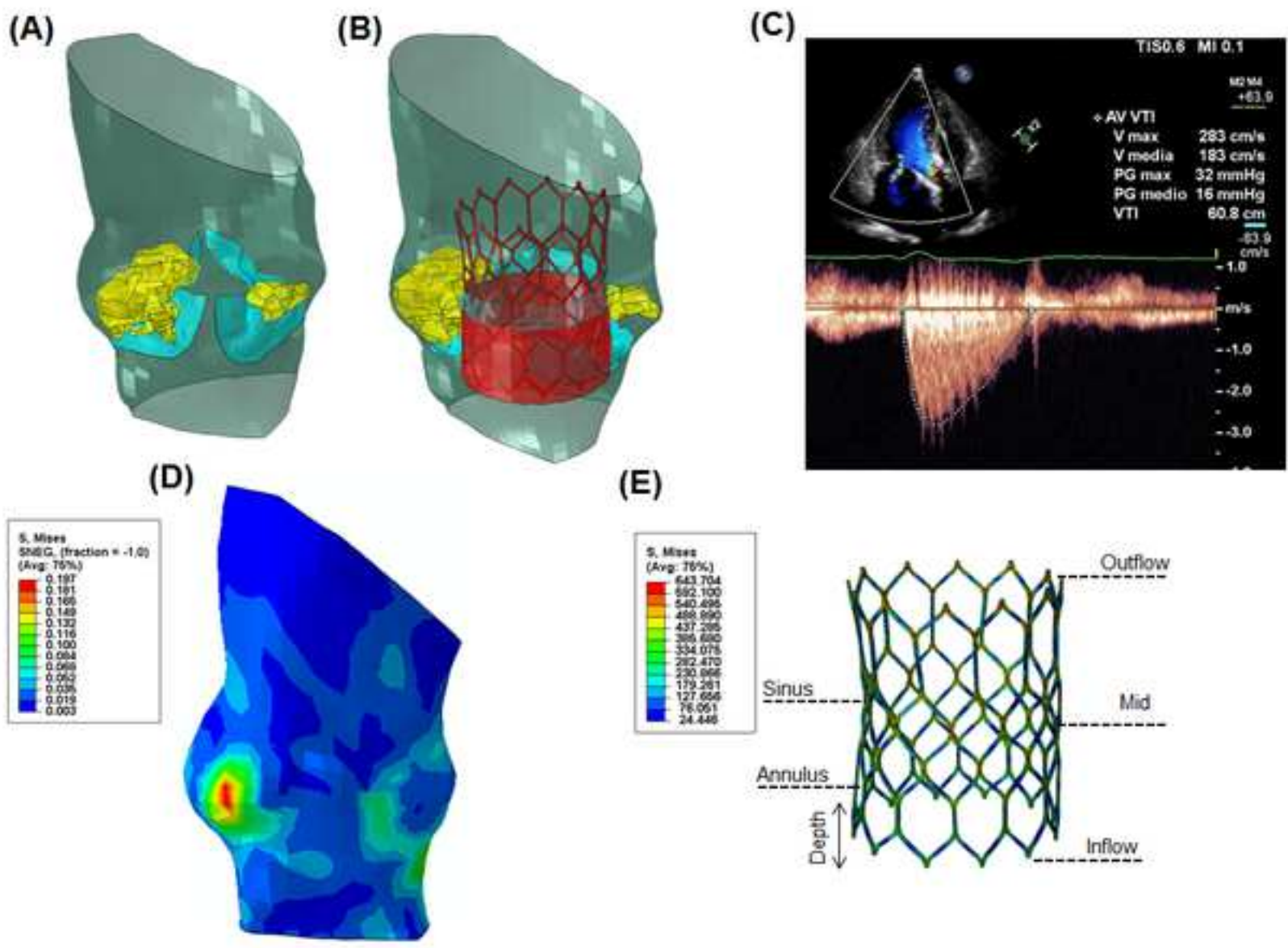
Table 3: Mises stress at annulus, mean depth of S3 implantation and PVL for each patient; PVL grade as: minimal <30 ml/s; moderate 30-59 ml/s and severe >60 ml/s

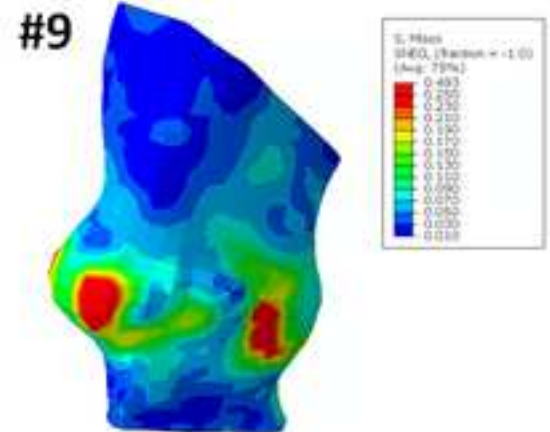
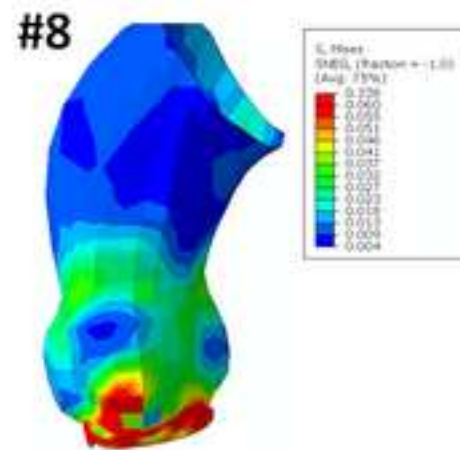
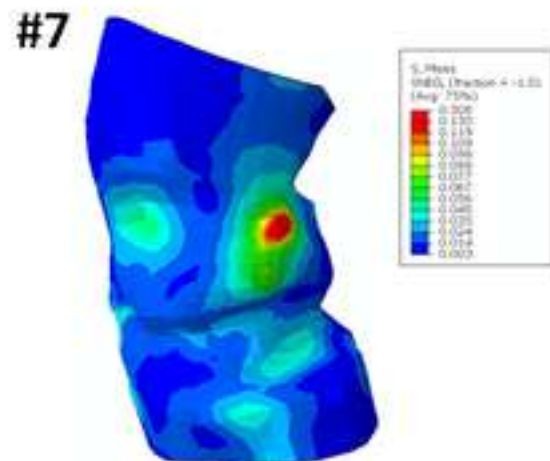
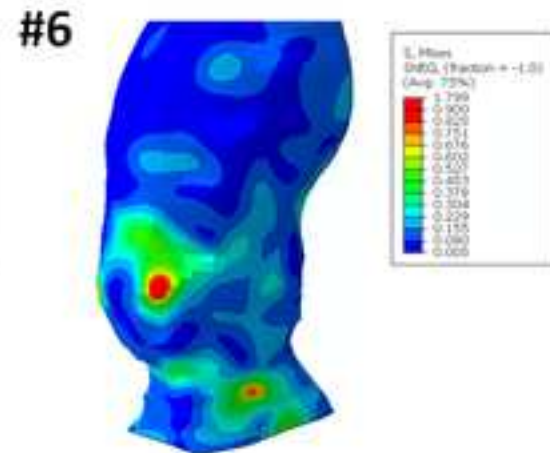
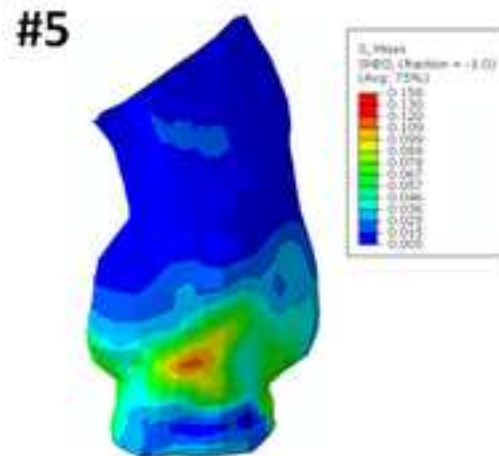
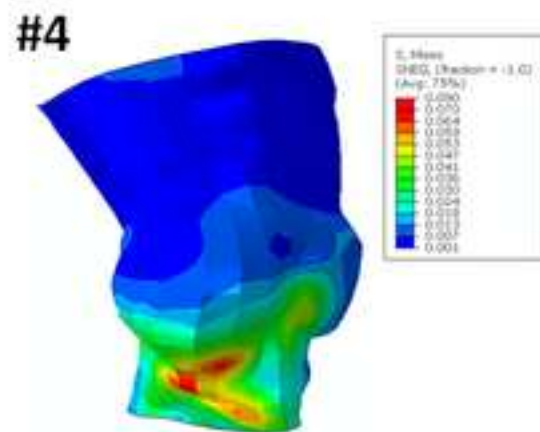
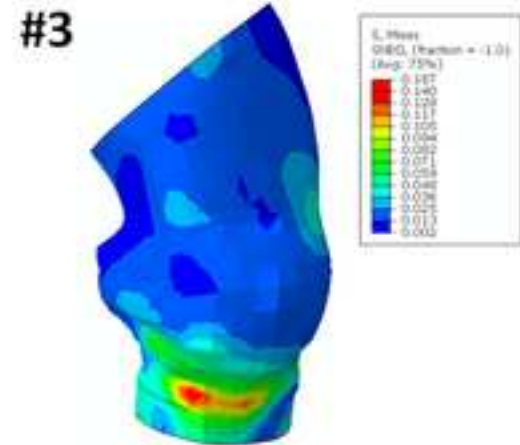
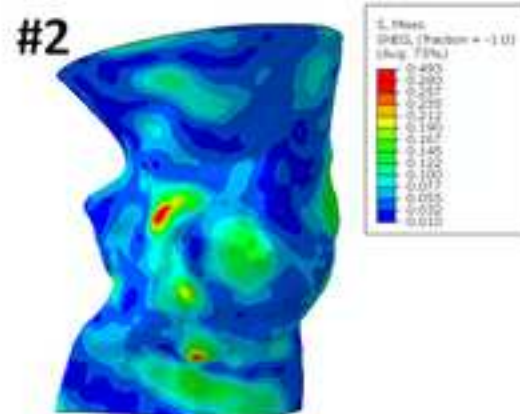
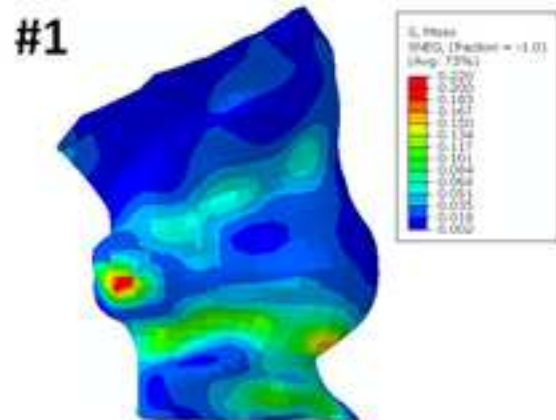
	#1	#2	#3	#4	#5	#6	#7	#8	#9
<i>Bicuspid Valve</i>	T1	T1	T1	T1	T1	T1	T2	T2	T1
<i>Device Size</i>	raphe	raphe	raphe	raphe			raphe	raphe	raphe
<i>Stress, MPa</i>	0.22	0.85	0.18	0.09	0.08	0.07	0.06	0.32	0.21
<i>SPH PVL, ml/s</i>	23.4	26.3	34.5	18.0	24.9	29.3	24.7	15.2	18.1
<i>TEE PVL, -</i>	min	min	mod	min	min	min	min	min	min
<i>Depth, mm</i>	5.5	5.2	5.8	3.1	4.6	5.8	4.7	5.9	8.9

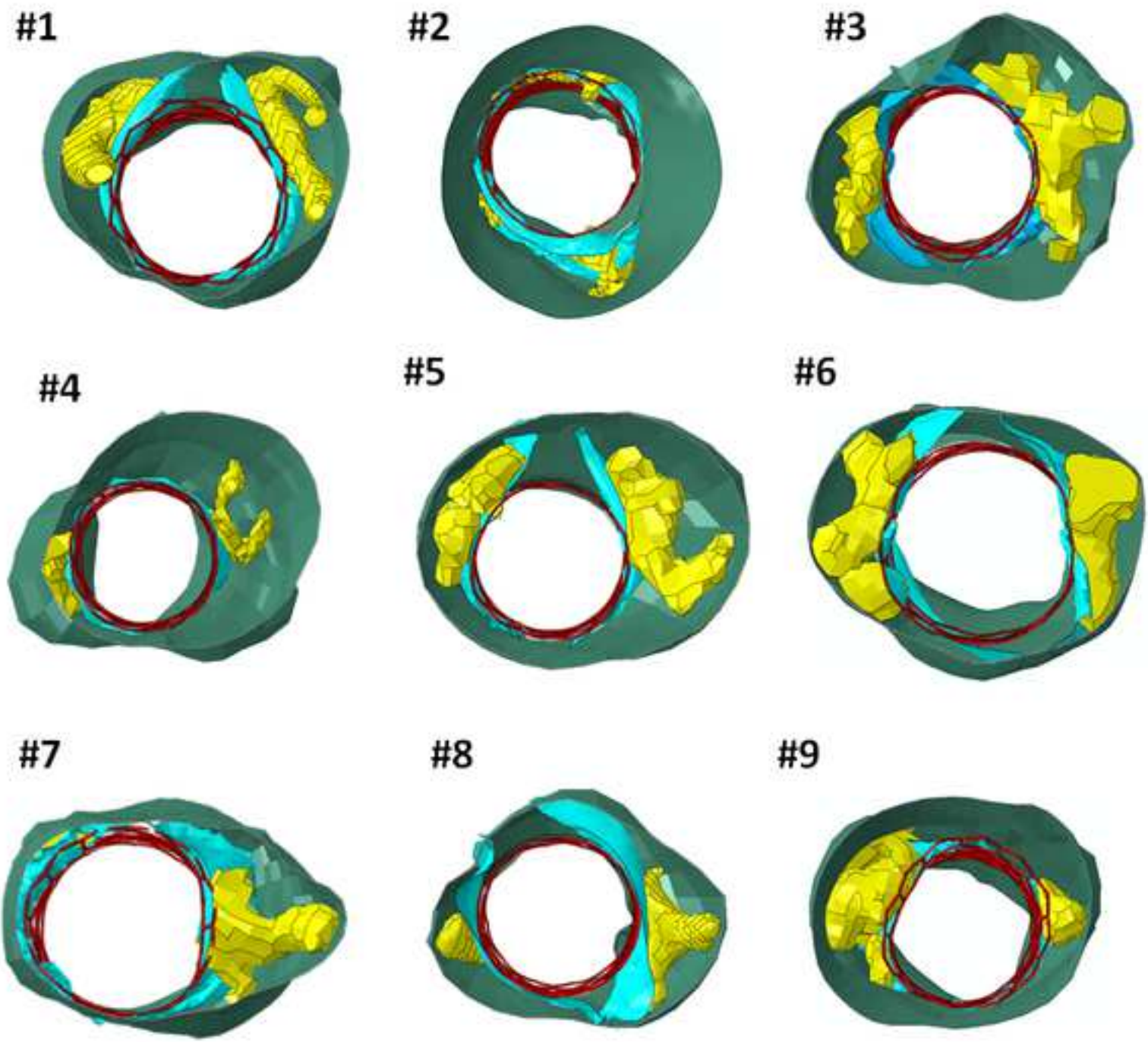


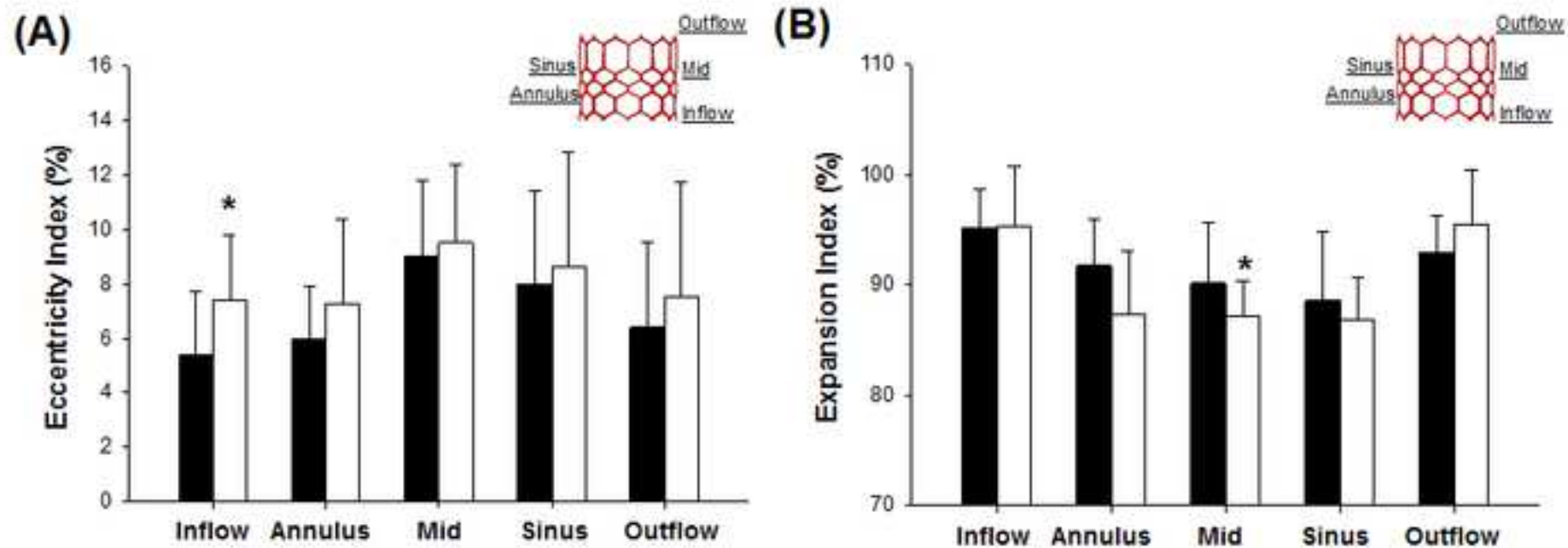


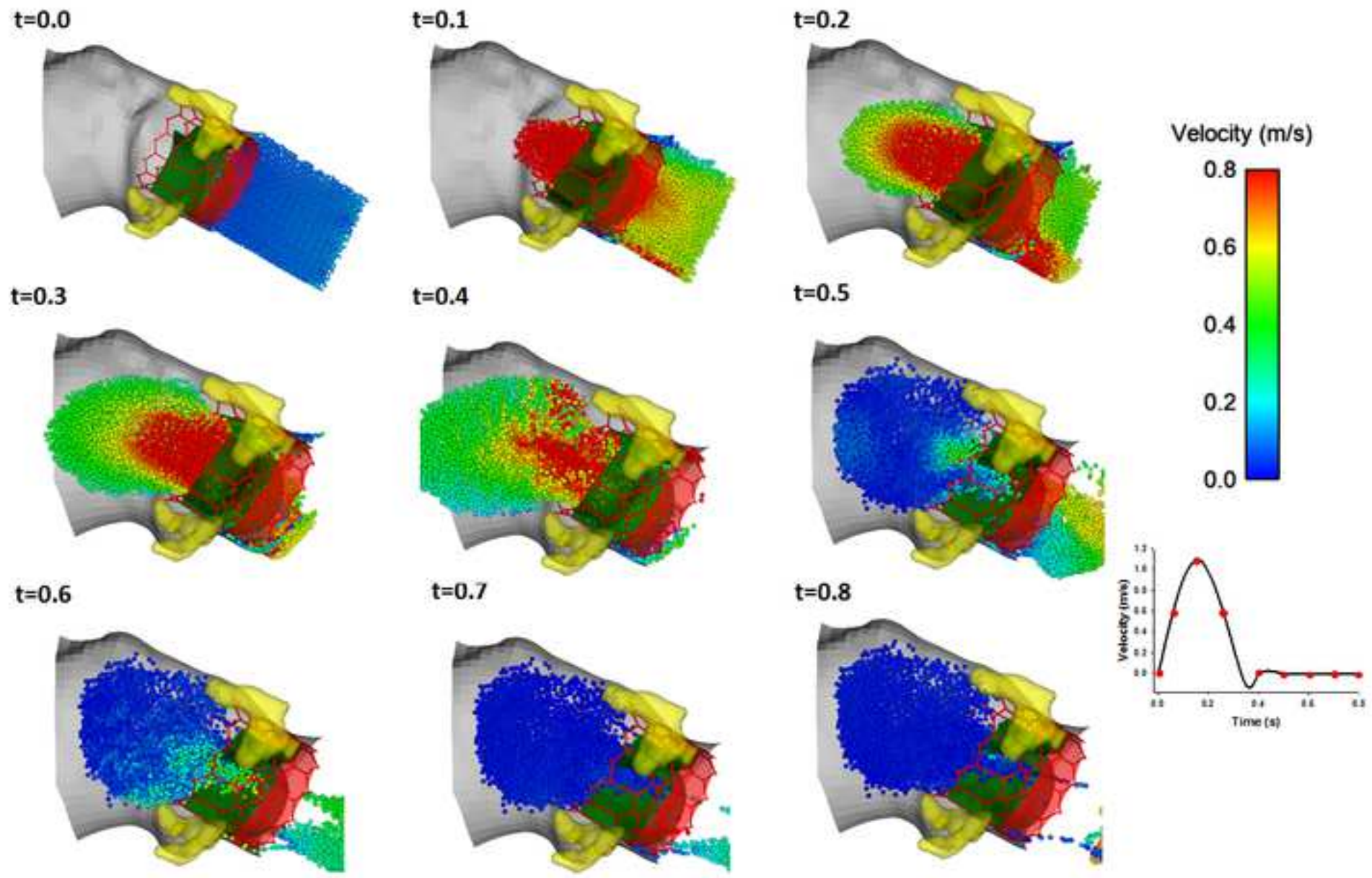


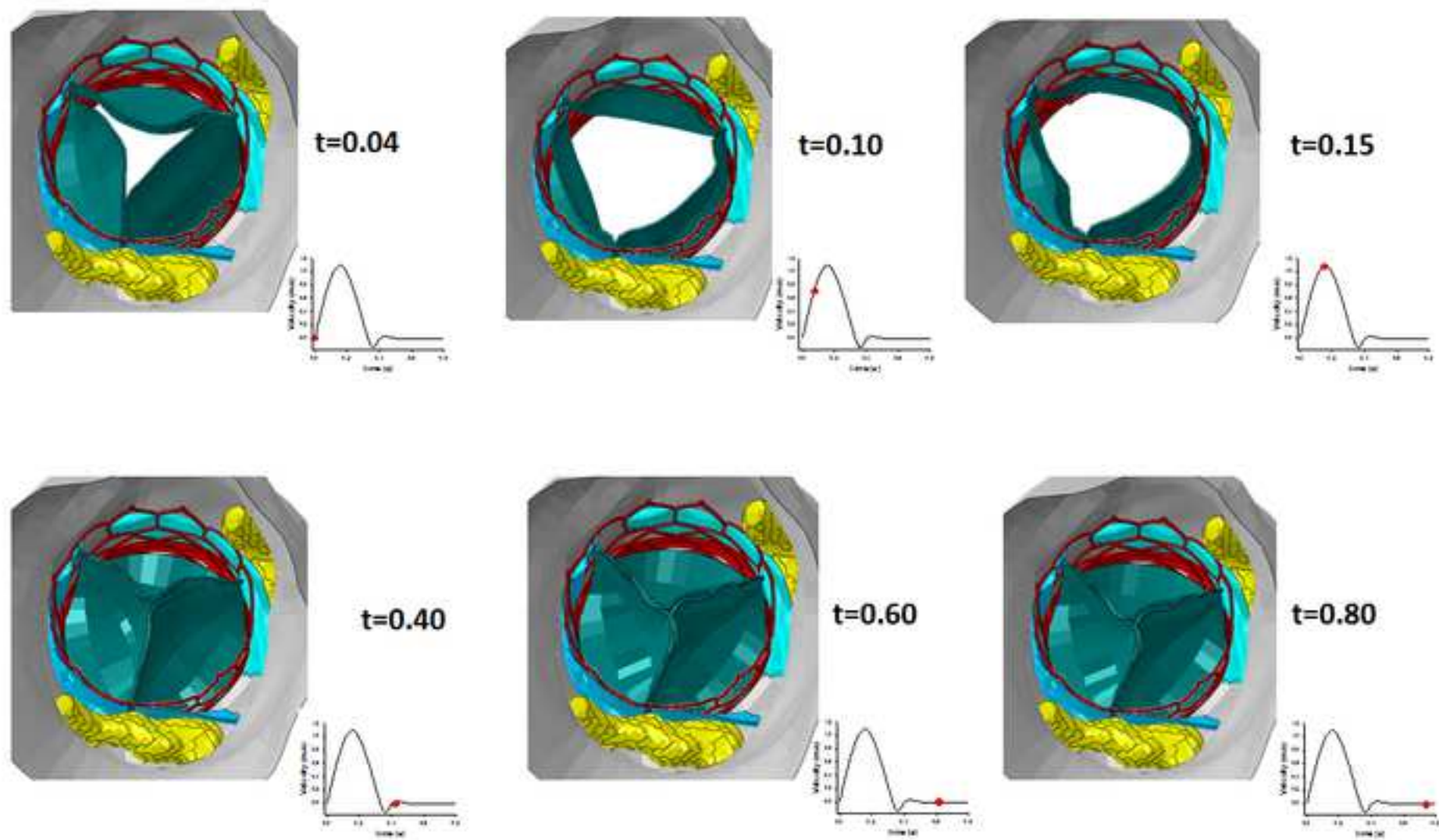












Biography

Salvatore Pasta, PhD, is Professor of Bioengineering at University of Palermo working on the cardiovascular biomechanics; specifically, the understanding of pathophysiology by modeling and experimental mechanics



Stefano Cannata, MD, is an interventional cardiologist at ISMETT IRCCS working on the replacement of diseased aortic and mitral valve with transcatheter heart valves



Giovanni Gentile, MD, is a radiologist at ISMETT IRCCS with high experience on heart CT and MR imaging. He worked on the measurements of deformed shape of transcatheter heart valve



Marzio Di Giuseppe, MEng, is a PhD student at University of Palermo using computational modeling to understand the mechanics of bicuspid aortic valve.



Federica Cosentino, MEng is a PhD student at University of Palermo worked on the development of patient-specific model by reconstruction of aortic root anatomy



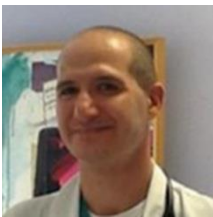
Francesca Pasta, MD, is a radiologist at University of Palermo with experience on the CT imaging of the bicuspid aortic valve. She performed the measurements of deformed shape of transcatheter heart valve



Valentina Agnese, PhD, is associate researcher at ISMETT IRCCS working as data manager. She performed the statistics and the data interpretation



Diego Bellavia, MD, PhD, is an attending cardiologist at ISMETT IRCCS with an outstanding experience in echocardiography. He performed the functional TTE imaging and data analysis



Giuseppe Raffa, MD, is a cardiac surgeon at ISMETT IRCCS and was involved on the data analysis and writing.



Michele Pilato, MD, is the chief the cardiac surgery group at ISMETT IRCCS and ahead of the Department for the Treatment and Study of Cardiothoracic Diseases and Cardiothoracic Transplantation at our hospital institution



Caterina Gandolfo, MD, is the chief of interventional cardiologists at ISMETT IRCCS and ahead of the TAVI program at our hospital institution. She was recipient of several national awards on TAVI.

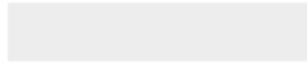


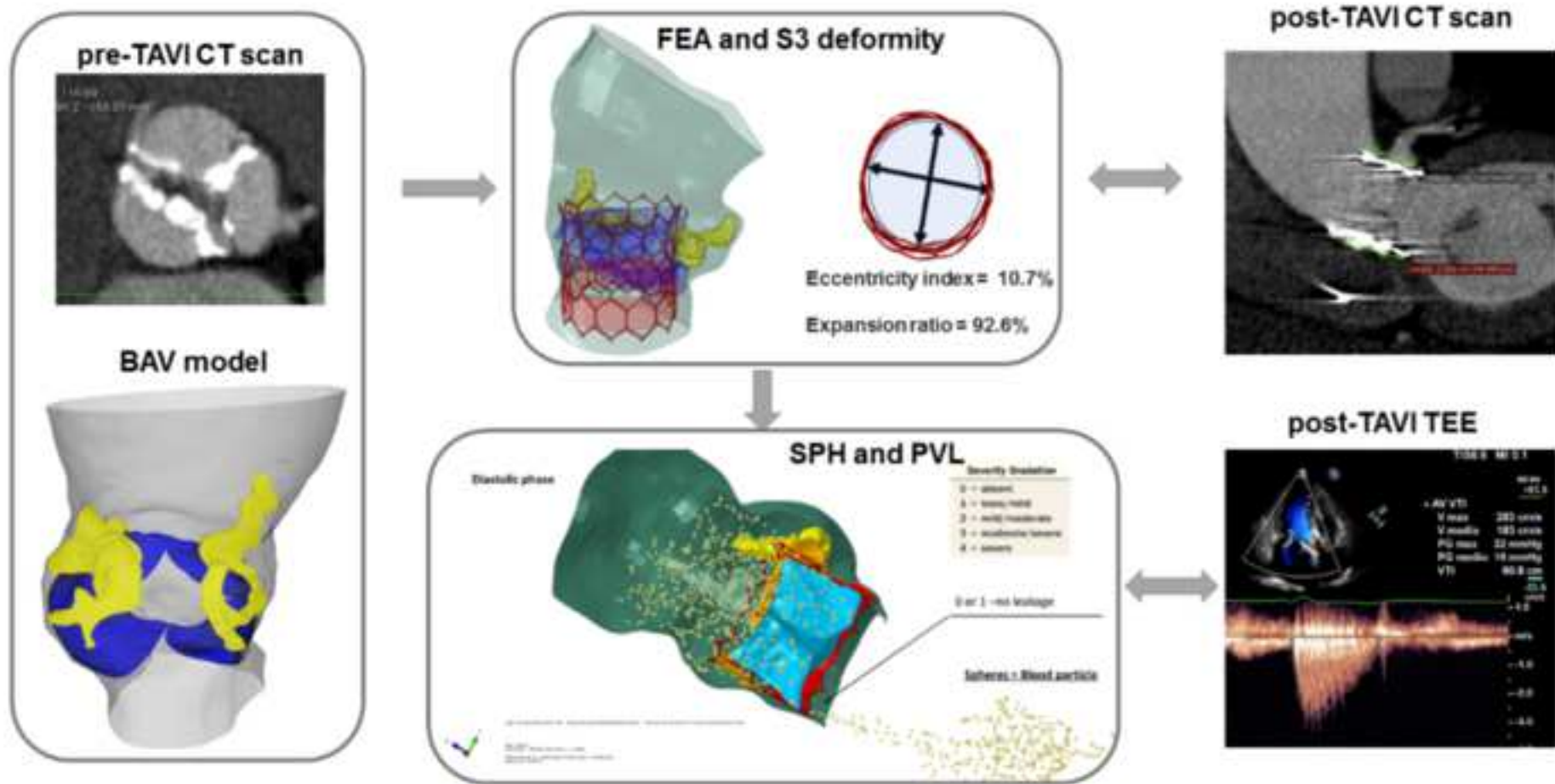


[Click here to access/download](#)

Supplementary material (videos/animations/long tables)

Movie 1.avi





Graphical Abstract: Computational framework of TAVI in patients with stenotic bicuspid aortic valve